

# Asymmetric supercapacitor based on controllable WO<sub>3</sub> nanorod bundle and alfalfa-derived porous carbon

*Kanjun Sun<sup>\*a</sup>, Fengting Hua<sup>b</sup>, Shuzhen Cui<sup>b</sup>, Yanrong Zhu<sup>a</sup>, Hui Peng<sup>b</sup>, Guofu Ma<sup>\*b</sup>*

<sup>a</sup>College of Chemistry and Environmental Science, Lanzhou City University, Lanzhou 730070, China

<sup>b</sup>Key Laboratory of Eco-Environment-Related Polymer Materials of Ministry of Education, Key Laboratory of Polymer Materials of Gansu Province, College of Chemistry and Chemical Engineering, Northwest Normal University, Lanzhou 730070, China

\*Corresponding authors. Tel./Fax.: +86 931 7975121

E-mailaddresses: Sunkj@lzcw.edu.cn (K. Sun), magf@nwnu.edu.cn (G. Ma).

## **S1. Materials Characterization**

The morphologies and structures of the samples were characterized by scanning electron microscopy (FE-SEM, Ultra Plus, Carl Zeiss, Germany). The Brunauer-Emmett-Teller surface areas (BET) of the samples were analyzed by nitrogen adsorption in a Micromeritics ASAP 2020 nitrogen adsorption apparatus (U. S. A.). The pore size distribution plots were recorded from the desorption branch of the isotherms based on the nonlocal density functional theory (NLDFT) model. Raman spectra was recorded with an in via Raman spectrometer (Renishaw) and X-ray diffraction (XRD) of samples was performed using a Rigaku D/Max-2400 diffractometer with Cu K $\alpha$  radiation ( $k = 1.5418 \text{ \AA}$ ) at 40 kV, 100 mA. The  $2\theta$  measure range was from  $5^\circ$  to  $80^\circ$ . X-ray photoelectron spectroscopy (XPS) measurement was performed on an Escalab 210 system (Germany).

## **S2. Electrochemical measurement**

The electrochemical properties of electrodes were analyzed by cyclic voltammetry (CV), galvanostatic charge/discharge (GCD) and electrochemical impedance spectroscopy (EIS) measurements in three-electrode system and two-electrode configuration was performed with an electrochemical workstation system (CHI660D, Shanghai Chen Hua Co. Ltd, China). The cycle-life stability was recorded was performed with cycling testing equipment (CT2001A, Wuhan Land Electronic Co. Ltd, China).

## **S3. Three-electrode system**

The three-electrode system was first used to evaluate the electrochemical properties of the different pH values of WO<sub>3</sub> and carbons materials in 1 M H<sub>2</sub>SO<sub>4</sub> aqueous electrolyte. The working electrode used a glassy carbon electrode with a diameter of 5 mm. The reference electrode and counter electrode were saturated calomel electrode (SCE) and a high purity carbon rod, respectively. The working

electrode is prepared as follows: typically, 4 mg of electrode materials were dispersed in 0.4 mL of 0.25 wt% Nafion ethanol solutions with assistance by ultrasonic vibration. Then, 8 mL of above suspension were dropped onto the glassy carbon electrode with a diameter of 5 mm as work electrode and dried for 10 min at room temperature.

The specific capacitances of the carbon or WO<sub>3</sub>-X sample were calculated from the charge-discharge curves based on the following equation:

$$C = I\Delta t / m\Delta V \quad (1)$$

where,  $C$  (F g<sup>-1</sup>) is the specific capacitance,  $I$  (A) refers to the discharge current,  $\Delta V$  (V) represents the potential change within the discharge time  $\Delta t$  (s), and  $m$  (g) corresponds to the total weight of the carbon and WO<sub>3</sub>-X.

#### **S4. Two-electrode system**

The APAC-2//WO<sub>3</sub>-2.0 asymmetric supercapacitor was assembled in 1 M H<sub>2</sub>SO<sub>4</sub> aqueous electrolyte using polygonal pseudo-capacitive materials WO<sub>3</sub>-X as the negative electrode, the porous carbon APAC-2 as positive electrode into sandwich-type cells construction. The positive and negative electrodes were pressed together and separated by a filter paper. The working electrode was prepared by mixing the active material with polyvinylidene fluoride (PVDF) and commercial carbon black (8:1:1) in N-methyl-2-pyrrolidone (NMP) until homogeneous slurry. The slurry was coated on stainless steel nets with a working area of 1.0 cm<sup>2</sup> and the electrodes were dried at 60 °C for 24 h and then weighted and pressed into sheets under 15 MPa. According the specific capacitance and potential range for the charge/discharge process at a current density of 1 A g<sup>-1</sup>, an ASC was constructed. The loading mass ratio of active materials  $m_{(APAC-2)/(WO_3-2.0)}$  was estimated to be 1.37. The mass loading is 5.38 mg and 4 mg for positive and negative electrode materials, respectively.

The cell capacitance ( $C_{cell}$ ), single electrode ( $C_s$ ), energy density ( $E$ ) and power density ( $P$ ) at different current densities are calculated based on these curves and using the following equations:

$$C_{cell} = I\Delta t / m\Delta V \quad (2)$$

$$C_s = 4 \times C_{cell} \quad (3)$$

$$E = C_{cell}\Delta V^2 / 2 \quad (4)$$

$$P = E / \Delta t \quad (5)$$

where  $C_{cell}$  ( $F g^{-1}$ ) is the specific capacitance of the ASC device,  $C_s$  ( $F g^{-1}$ ) is the specific capacitance of the single electrode,  $I$  (A) represents the discharge current,  $m$  is the total mass of the active materials in both electrodes,  $\Delta t$  (s) is the discharge time;  $\Delta V$  (V) refers to the voltage window,  $E$  ( $Wh kg^{-1}$ ) corresponds to the energy density and  $P$  ( $W kg^{-1}$ ) is the power density.

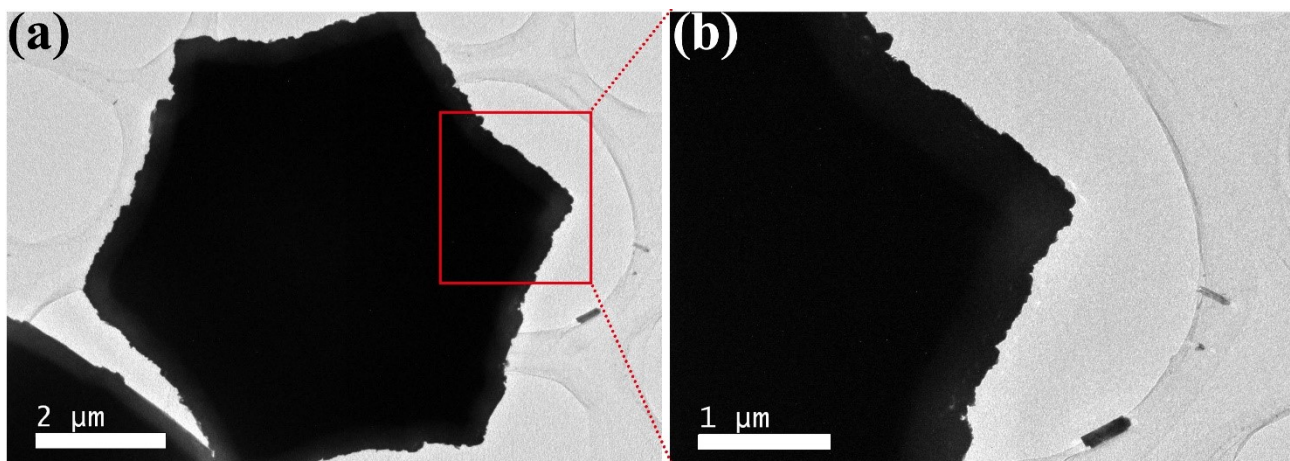


**Figure S1.** (a, b) TEM image of the  $\text{WO}_3$ -2.0 nanorod bundle.

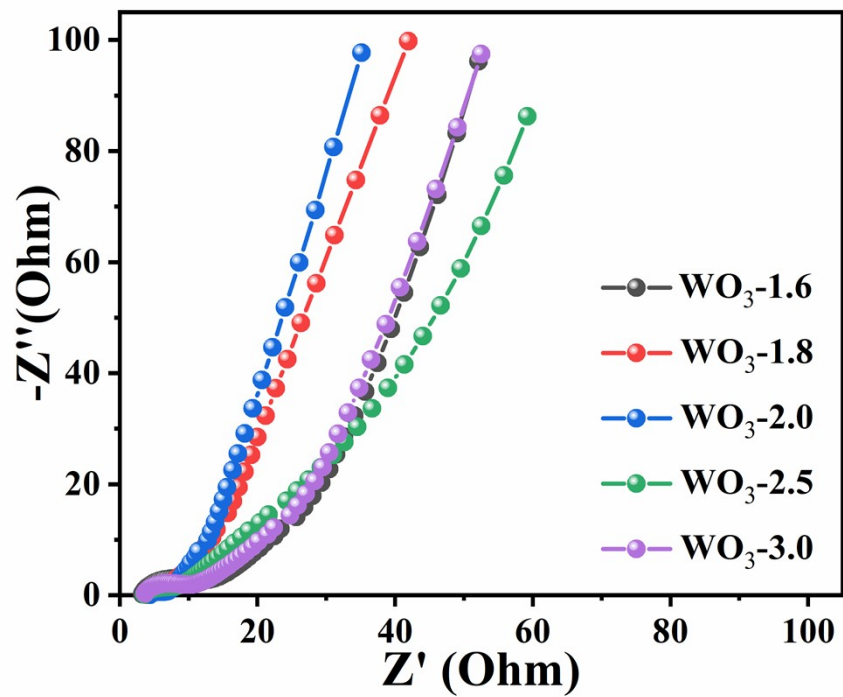


**Figure S2.** Nyquist plots of the WO<sub>3</sub>-X series samples.

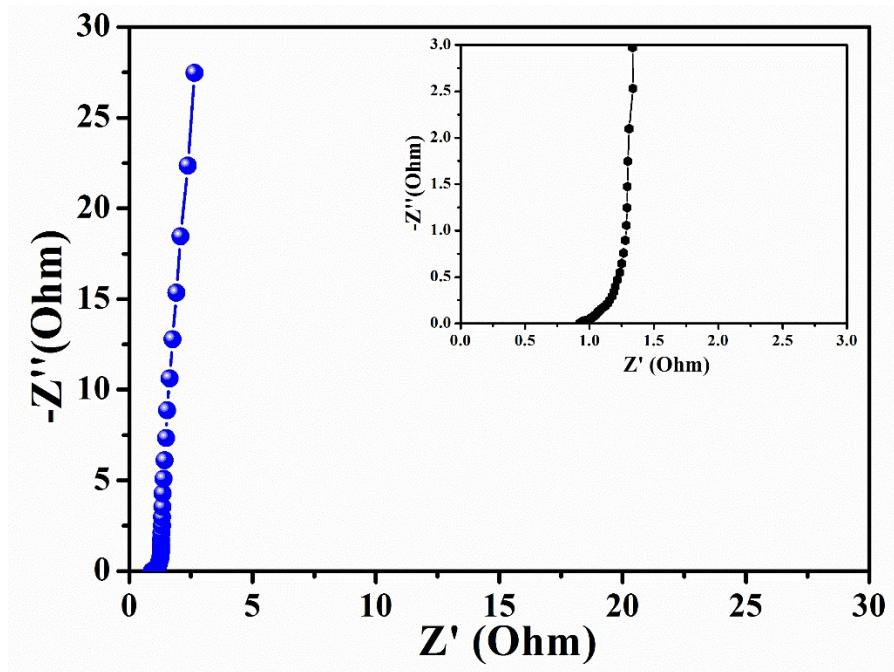


**Figure S3.** Nyquist plots of the APAC-2 and its expanded high frequency region (inset).

**Table S1.** Performance comparison of symmetric cells used various carbon materials in the references.

Carbon-based materials	Specific surface area (m <sup>2</sup> g <sup>-1</sup> )	Average pore diameter (nm)	Specific capacitance (three electrodes)	Capacity rate performance	References
Nitrogen-doped carbon nanofiber (N-CNFs-900)	562.51	3.64	202 F g <sup>-1</sup> at 1 A g <sup>-1</sup>	81.7% (30 A g <sup>-1</sup> )	[Ref. S1]
AQ-modified CC2 (1-AAQ-CC2)	1214.1	2.8	328 F g <sup>-1</sup> at 0.5 A g <sup>-1</sup>	75% (20 A g <sup>-1</sup> )	[Ref. S2]
Sorghum stalk based porous carbons (SSC1.0)	1354.7	2.26	216.5 F g <sup>-1</sup> at 0.5 A g <sup>-1</sup>	75% (8 A g <sup>-1</sup> )	[Ref. S3]
Nitrogen-doped pomelo mesocarp carbon (N-PMNC)	974.6	2.9	245 F g <sup>-1</sup> at 0.5 A g <sup>-1</sup>	72% (20 A g <sup>-1</sup> )	[Ref. S4]
Alfalfa-derived porous activated carbon (APAC-2)	1576.3	3.336	262.1 F g <sup>-1</sup> at 0.5 A g <sup>-1</sup>	70.2% (10 A g <sup>-1</sup> )	This Work



## References

- [S1] L. Chen, X. Zhang, H. Liang, M. Kong, Q. Guan, P. Chen, Z. Wu, S. Yu, Synthesis of nitrogen-doped porous carbon nanofibers as an efficient electrode material for supercapacitors, *ACS Nano*, 2012, **6**, 7092.
- [S2] G. Ma, F. Hua, K. Sun, E. Feng, Z. Zhang, H. Peng, Z. Lei, Anthraquinones-modified porous carbon as composite electrode for symmetric supercapacitor, *Ionics*, 2018, **24**, 549-561.
- [S3] G. Ma, F. Hua, K. Sun, Z. Zhang, E. Feng, H. Peng, Z. Lei, Porous carbon derived from sorghum stalk for symmetric supercapacitors, *RSC Adv.*, 2016, **6**, 103508-103516.
- [S4] H. Peng, G. Ma, K. Sun, Z. Zhang, Q. Yang, Z. Lei, Nitrogen-doped interconnected carbon nanosheets from pomelo mesocarps for high performance supercapacitors, *Electrochim. Acta*, 2016, **190**, 862–871.